Nonlinear Analysis of Active Aperture Coupled Reflectarray Antenna Containing Varactor Diode

I. Aryanian, A. Abdipour, and G. Moradi

Department of Electrical Engineering
Amirkabir University of Technology, Tehran, 15914, Iran
iman_aryanian@aut.ac.ir, abdipour@aut.ac.ir, ghmoradi@aut.ac.ir

Abstract ─ Radiation pattern of reflectarray antenna can be controlled using varactor diode in the antenna structure, but may cause nonlinear response. Thus, it is needed to design active reflectarray antenna considering nonlinear behavior of the unit cell. However, in the past papers, active element of varactor tuned reflectarray antenna is assumed linear, while in this paper, nonlinear analysis of active reflectarray antenna is explained and an active aperture coupled reflectarray unit cell containing two varactor diodes is analyzed. Harmonic balance method is used in analyzing active unit cell using nonlinear model of the diode. Therefore, this paper shows the significance of nonlinear analysis of active reflectarray antenna, and also the effect of nonlinear element in radiation pattern is presented. By the explained method, the impact of nonlinearities on performance of reflectarrays can be investigated. Furthermore, any active reflectarray cell having active device by any nonlinear model can be used in the analysis, and the impact of parameters of the model can be studied.

Index Terms ─ Active antenna, beam forming, nonlinear analysis, reflectarray antenna, steerable antenna.

I. INTRODUCTION

A microstrip reflectarray antenna is a low profile planar reflector that consists of microstrip patch arrays printed on a dielectric substrate which its surface is illuminated by a feed antenna. Each element of the array is designed to produce required reflection phase shift to form a desired pattern. The phase can be controlled by active element which gives the capability of controlling the pattern [1,2]. Different methods are used to add reconfigurability to reflectarray antenna, using microstrip elements with an integrated electronic control, like MEMs-based structures [3], varactor loaded patches [4,5], PIN diodes [6] or liquid crystal based structures [7]. Varactor tuned reflectarray elements may be able to control phase of the unit cell continuously over a 360 degrees range.

Harmonic balance analysis of nonlinearly loaded antennas is reported in the past papers [8,9] but it is not explained for reflectarray antenna. Nonlinear analysis of active reflectarray antenna is essential when radiated power of the antenna is such that active elements behave nonlinear. In this paper, it is shown that power distribution on the antenna surface may cause some active elements of antenna to behave nonlinear. In these cases, unit cell of active reflectarray antenna should be analyzed in a two-step process to consider nonlinear behavior of active element. First, passive radiation part should be simulated by full wave analysis method to obtain parameters of the passive part. For this purpose, unit cell of the antenna is simulated assuming infinite array and the active element is replaced by a two port network. Also, two spatial ports are considered for each polarization of incident plane wave which are modelled as Floqute port. Next, obtained scattering parameters are used in nonlinear analysis of the unit cell. This process is carried out in this paper for an active unit cell in the centre frequency of 5.4 GHz where the unit cell has two varactor diodes. Nonlinear results are used in designing a sample reflectarray antenna.

II. UNIT CELL CONFIGURATION

Aperture coupled microstrip antenna have been used for single or dual linear polarization reflectarrays [10,11]. In this structure, each cell consists of a microstrip line coupled to the radiating patch on the opposite side of the substrate via an aperture in the ground plane as shown in Fig. 1. The unit cell contains two varactor diodes as shown in Fig. 1. Parameters of the unit cell are borrowed from [4] to compare its test results by this paper where relative dielectric constant for 1 mil substrate is 3.4, and for line substrate is 2.2. The patch is separated from the ground plane and slot by a 3-mm thick foam with a relative dielectric constant of 1.11. Other parameters of the unit cell are given in Table 1. Unit cell is designed for the center frequency of 5.4 GHz.
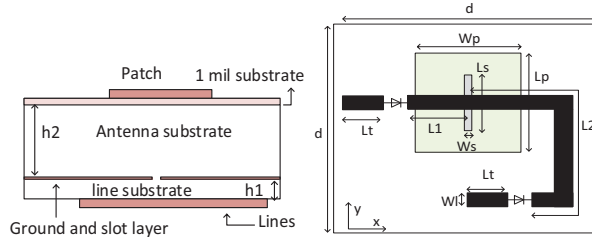
Fig. 1. Antenna unit cell schematic.

Table 1: Unit cell parameters

Parameter	Value	Parameter	Value
Lp	19.5 mm	Wp	15.5 mm
h1	0.5 mm	Ls	15.4 mm
Ws	0.76 mm	Wl	1.5 mm
h2	3 mm	d	35 mm
L2	16.1 mm	L1	6 mm
Lt	7.8 mm		

III. UNIT CELL MODELING

To simulate the unit cell assuming infinite array, active elements are replaced by two port networks. The unit cell is modelled as a six port network as shown in Fig. 2, in which ports 5 and 6 are spatial ports modeled as Floqute port, and ports 1 to 4 are located in the transmission line. After modeling the linear part of the unit cell, active elements are added to the analysis by nonlinear two port networks as shown in Fig. 2.

Parameters of the varactor diodes used in this work are given in Table 2, and nonlinear diode model is shown in

Fig. 3, which has one nonlinear capacitance and one nonlinear current source. C_p and L_p are parasitic capacitance and inductance of the model. Also, R_s is series ohmic resistance, $C_j(v)$ is the nonlinear junction capacitance, and $R_j(v)$ is the nonlinear junction impedance of the model.
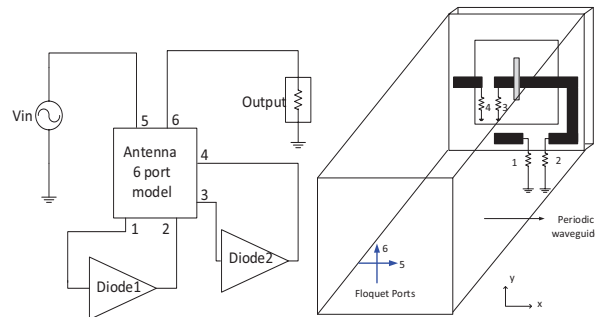

Fig. 2. Six port modelling of the unit cell.

Table 2: Diode parameters

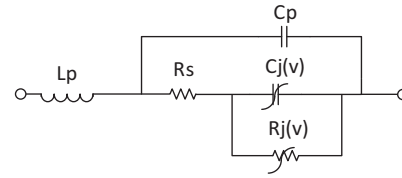| Symbol	Quantity	Value
Is	Saturation current	100 (pA)
N	Ideal factor	2
Vt	Thermal voltage	26 (mV)
Cj0	Junction capacitance	1.7 (pF)
M	Grading coefficient	0.9
vj	Junction potential	1.2
Fc	Forward-bias depletion capacitance coefficient	0.5
LP	Parasitic inductance	0.4 (nH)
CP	Parasitic capacitance	0.1 (pF)
Rs	Ohmic resistance	0.9 (Ohm)

Fig. 3. Nonlinear model of the diode.

Current source of the model is given as [12]:

$$I_d = \begin{cases} I_s\left(e^{v_d/NV_t}-1\right), & v_d \geq -10NV_t \\ I_s\left(e^{-10}-1\right)+\dfrac{I_s}{NV_t}e^{-10}\left(v_d+10NV_t\right), & v_d < -10NV_t \end{cases}. \quad (1)$$

As well, electric charge is expressed as:

$$Q_j = \begin{cases} \dfrac{V_jC_{j0}}{1-M}\left(1-\left(1-\dfrac{v_d}{V_j}\right)^{1-M}\right), & v_d \leq F_cV_j \\ \dfrac{C_{j0}}{(1-F_c)^M}[v_d+\dfrac{M}{V_j(1-F_c)}\left(\dfrac{v_d^2}{2}-V_jF_cv_d\right)], & v_d > F_cV_j \end{cases}. \quad (1)$$

Besides, capacitance of the model is obtained as:

$$C_j = \begin{cases} C_{j0}\left(1-\dfrac{v_d}{V_j}\right)^{-M}, & v_d \leq F_cV_j \\ \dfrac{C_{j0}}{(1-F_c)^M}\left[1+\dfrac{M}{V_j(1-F_c)}\left(v_d-V_jF_c\right)\right], & v_d > F_cV_j \end{cases}, \quad (2)$$

where v_d is voltage of diode, C_{j0}, M, N, F_c, V_j, I_s are parameters of the diode model and V_t is 26 mV.

IV. NONLINEAR ANALYSIS

The nonlinear analysis of the unit cell is performed using harmonic balance method [13]. Hence, the unit cell is divided into nonlinear and linear networks as shown in
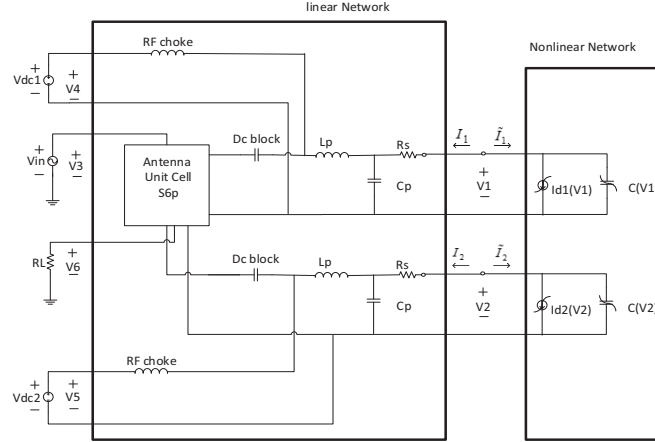
Fig. 4.

Fig. 4. Dividing the unit cell to nonlinear and linear networks.

The nonlinear network is composed of nonlinear capacitances and nonlinear current sources and the linear network consists of parasitic elements and lumped elements of the unit cell, and also 6-port network of the unit cell obtained in the previous section. Our aim is to find voltages of V_1 and V_2 of

Fig. 4, to have $I_1 + \tilde{I}_1 = 0$, and $I_2 + \tilde{I}_2 = 0$.

A. Currents of the linear part

Current of the linear subcircuit can be expressed as:

$$\begin{bmatrix} I_1 \\ I_2 \\ \vdots \\ I_6 \end{bmatrix} = \begin{bmatrix} Y_{11} & Y_{12} & \cdots & Y_{16} \\ Y_{21} & Y_{22} & \cdots & Y_{26} \\ \vdots & \vdots & \vdots & \vdots \\ Y_{61} & Y_{62} & \cdots & Y_{66} \end{bmatrix} \begin{bmatrix} V_1 \\ V_2 \\ \vdots \\ V_6 \end{bmatrix}. \tag{3}$$

Partitioning the Y matrix in (4) gives an expression for I, the vector of currents of linear part in ports 1 and 2:

$$I = \begin{bmatrix} I_1 \\ I_2 \end{bmatrix} = \begin{bmatrix} Y_{11} & Y_{12} \\ Y_{21} & Y_{22} \end{bmatrix} \begin{bmatrix} V_1 \\ V_2 \end{bmatrix} +$$

$$\begin{bmatrix} Y_{13} & Y_{14} & Y_{15} \\ Y_{23} & Y_{24} & Y_{25} \end{bmatrix} \begin{bmatrix} V_3 \\ V_4 \\ V_5 \end{bmatrix} = Y_L.V + Y_S.V_S. \tag{4}$$

$I_S = Y_S V_S$ represents a set of current sources in parallel with the first and second ports; which transforms the input and output port excitations into this set of current sources.

B. Currents of the nonlinear part

Fourier transforming the charge waveform at each port gives the charge vectors for the capacitors at each port:

$$F\{q_1(t)\} \rightarrow Q_1, \quad F\{q_2(t)\} \rightarrow Q_2, \tag{5}$$

and the charge vector, Q, is:

$$Q = \begin{bmatrix} Q_1 \\ Q_2 \end{bmatrix}. \tag{6}$$

The nonlinear-capacitor current is the time derivative of the charge waveform. Taking the time derivative corresponds to multiplying by jω in the frequency domain, so:

$$i_c(t) = \frac{dq(t)}{dt} \leftrightarrow jk\omega_P Q \qquad k = 0,1,\ldots,K$$

$$\Rightarrow I_c = j\Omega Q, \tag{7}$$

where Ω is a diagonal matrix with 2 cycles of $0, \omega_0, \ldots, k\,\omega_0$ along the main diagonal where k=3 is the number of harmonics determined.

Fourier transforming from nonlinear current vector in time domain gives the nonlinear current vector in frequency domain:

$$F\big(i_{d1}(t)\big) \rightarrow I_{d1}, \quad F\big(i_{d2}(t)\big) \rightarrow I_{d2}. \tag{8}$$

Therefore, vector of nonlinear current sources in ports 1 and 2, I_G is:

$$I_G = \begin{bmatrix} I_{d1} \\ I_{d2} \end{bmatrix}. \tag{9}$$

So, nonlinear current vector of ports 1 and 2 is $\tilde{I} = I_G + I_C$.

Calculating the admittance parameters of linear network of

Fig. 4, which is a 6×6 matrix obtained using ADS simulation, the following harmonic balance equation is obtained [13]:

$$F(v) = I_s + Y_L.V + j\Omega Q + I_G = 0. \tag{10}$$

In this equation, $y_{m,n} = diag(y_{m,n}(k\,\omega_c))$, and V is the vector of nonlinear voltages of the nonlinear ports. Harmonic balance equation can be solved with different methods, among which the Newton-Raphson [13] technique is the most common technique and is used in this paper. Newton-Raphson technique is an

iterative method involving calculation of Jacobian matrix, which contains derivatives of all components of the vector $F(v)$, with respect to the components of V.

To obtain S_{11} parameter which shows the reflection from the unit cell in the same polarization with the incident field, LSSP simulation is used in ADS simulation. The LSSP simulation (Large-Signal S-Parameter Simulation) in the simulation-LSSP palette of ADS software, computes S-parameters for nonlinear circuits such as those that employ power amplifiers and mixers. In the latter case, S-parameters can be computed across frequencies, that is, from the RF input to the IF output. LSSP simulation is based on the harmonic balance simulation and uses harmonic balance techniques.

The port which the reflection coefficient should be calculated from it in the written harmonic balance code by MATLAB software, is considered as the input port. Then, voltage and current at this port is evaluated by running harmonic balance code.

In the next step, voltage of the input port V_{in} is obtained and input impedance from this port is calculated as:

$$Z_{in}(\omega_0) = \frac{V_{in}(\omega_0)}{I_{in}(\omega_0)}. \qquad (11)$$

Now S_{11} is evaluated by:

$$S_{11}(\omega_0) = \frac{Z_{in}(\omega_0) - Z_0}{Z_{in}(\omega_0) + Z_0}. \qquad (12)$$

Phase and amplitude of the S_{11} shows the reflected signal from the unit cell in the same polarization with the incident field. Considering nonlinear diode model and harmonic balance analysis, amplitude response and phase shift of the reflected signal from the cell for different power levels are obtained as shown in Fig. 5 and

Fig. 6, in which nonlinear result of harmonic balance analysis is verified by ADS simulation.
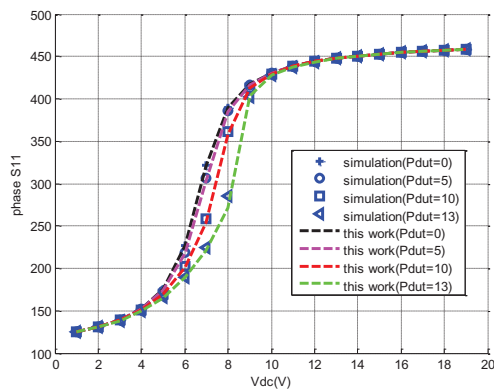

Fig. 5. Phase response of the active unit cell by nonlinear analysis.
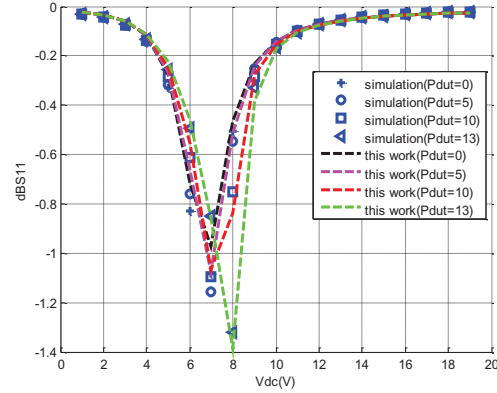

Fig. 6. Amplitude response of the active unit cell by nonlinear analysis.

Simulation results show that reflection phase and amplitude depend on the incident power. As the power increases, rectification and harmonics of the fundamental frequency starts to appear. This causes the reflection phase curves to be different from the ones obtained at a low power and the losses to increase. For high power levels, nonlinear behavior such as rectification occurs in the positive excursion of the RF signal when the reverse bias voltage is set to low values because of diode conduction. This rectification affects the reflection coefficient as can be seen in

Fig. 6. Besides, Fig. 5 shows that reflection phase is different from that of linear analysis. The maximum error of reflection phase in Fig. 5 is about 120 degrees which occurs in bias voltage of 8 (V), which shows that nonlinear phenomenon cannot be neglected. The unit cell is fabricated and tested in [4] and measurement results show this nonlinear behavior but nonlinear analysis is not performed in [4]. Test results of [4] are close to the results of this paper. However, because the parameters of the diode model is not specified in [4], the selected parameters for the varactor diode in this paper is different, and this leads to different cell response.

V. SAMPLE ACTIVE REFLECTARRAY DESIGN

To simulate the active antenna, a 31.5 cm × 31.5 cm antenna is designed using the explained unit cell by focal length of 39 cm in the frequency of 5.4 GHz. Assuming center of reflectarray as center of Cartesian coordinates, feed antenna is placed in (0, 0, 39 cm). First step to design the antenna is to find required phase shift of each cell to have a focused beam in a desired direction. Considering our antenna has N reflecting elements that are illuminated by a feed located at the focal point of the antenna, the excitation terms are proportional to the magnitude and phase of the electric

field at the nth patch. The feed has a certain angular taper over the antenna surface which can be included in the pattern analysis by multiplying the relative complex excitation term by a raised cosine factor [14], that can be adjusted to match the pattern of the actual feed by choosing the proper q, which is the exponent of the feed pattern function represented by $\cos^q \theta$ and is determined from the taper factor at the edges of the reflectarray, which is about -10 dB for a focused beam [14]. The angular taper of the feed can be modelled as $\dfrac{e^{-jkR_n}}{R_n}\cos\theta_n^q$. Consequently, by multiplying the complex excitation term by the compensating phase and amplitude factor $A_n e^{-jk\psi_n}$ resulted from each element, the complex reflected field from each element can be expressed in the form:

$$A_n \frac{\cos\theta_n^q}{|R_n|} e^{-j(kR_n-\psi_n)}, \tag{13}$$

in which ψ_n is the compensation phase of the nth element and (R_n) is the distance between the feed phase center and the nth element phase center. The required phase shift at each element to produce a collimated beam in a given direction is [14]:

$$\psi_n = k_0(R_n - (x_n\cos\phi_b + y_n\sin\phi_b)\sin\theta_b), \tag{14}$$

where θ_b, ϕ_b shows the beam direction, k_0 is the free space propagation constant, and (x_n, y_n) is the coordinates of element n.

Gain of the antenna can be computed using the input power of the feed horn P_F, according to:

$$G(\theta,\varphi) = \frac{4\pi r^2}{2\eta_0 P_F} |E(\theta,\varphi)|^2, \tag{15}$$

where η_0 is the intrinsic impedance of the free space and $|E(\theta,\varphi)|$ is the amplitude of the far electric field. Hence, far electric field should be calculated to obtain gain of the antenna which is explained in [14].

If nonlinear behavior of unit cell is not considered, the errors in the amplitude and phase of the reflected signal from each cell may reduce the gain. Antenna directivity with and without considering the nonlinear effect of active elements is shown in Fig. 8 and Fig. 9. In Fig. 8, feed power is so that some cells are in nonlinear region. Power distribution of the antenna for this scenario is shown in Fig. 7. In this case, considering amplitude and phase nonlinear behavior of the unit cell shown in Fig. 5 and Fig. 6, nonlinear analysis shows degradation in gain which cannot be assessed by linear analysis. In another scenario in Fig. 9, feed power is so that all cells are in linear region, where linear and nonlinear simulations have the same result. So, when feed power

is below 0 dBm, it is not necessary to consider the nonlinear effects. However, to assess the pattern of the active reflectarray antenna correctly, for all feed power, the nonlinear behavior of active element should be considered.
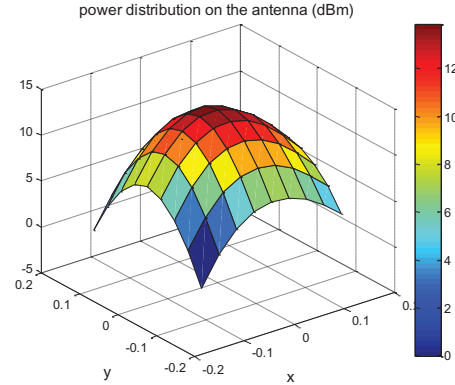

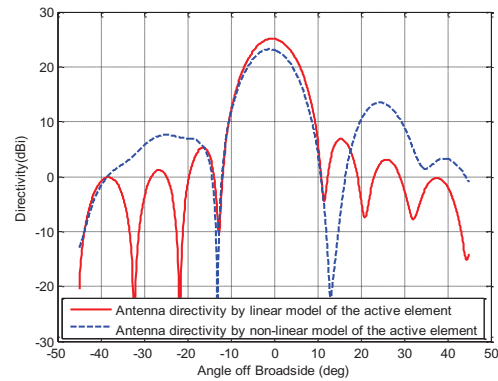Fig. 7. Supposed power on the antenna surface.

Fig. 8. Antenna directivity with and without considering the nonlinear effect of active elements when feed power is so that some cells are in nonlinear region.
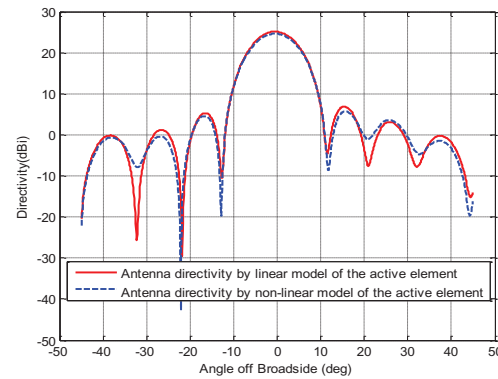

Fig. 9. Antenna directivity with and without considering the nonlinear effect of active elements when feed power is so that all cells are in linear region.

VI. CONCLUSION

Active reflectarray antenna containing varactor diode has been analysed considering nonlinear performance of the active element. The unit cell has been divided into two linear and nonlinear parts. Scattering parameters of the linear part is obtained using HFSS software and used in the harmonic balance analysis. A sample active reflectarray antenna has been designed which shows the error in predicting the pattern of the antenna with linear modeling of the active element.

REFERENCES

[1] T. Makdissy, R. Gillard, E. Fourn, E. Girard, and H. Legay, "Phase-shifting cell for dual linearly polarized reflectarrays with reconfigurable potentialities," 2013.

[2] F. Venneri, S. Costanzo, and G. Di Massa, "Design and validation of a reconfigurable single varactor-tuned reflectarray," *Antennas and Propagation, IEEE Transactions on*, vol. 61, pp. 635-645, 2013.

[3] O. Bayraktar, O. A. Civi, and T. Akin, "Beam switching reflectarray monolithically integrated with RF MEMS switches," *Antennas and Propagation, IEEE Transactions on*, vol. 60, pp. 854-862, 2012.

[4] M. Riel and J. Laurin, "Design of an electronically beam scanning reflectarray using aperture-coupled elements," *Antennas and Propagation, IEEE Transactions on*, vol. 55, pp. 1260-1266, 2007.

[5] F. Venneri, S. Costanzo, and G. Di Massa, "Reconfigurable aperture-coupled reflectarray element tuned by single varactor diode," *Electronics Letters*, vol. 48, pp. 68-69, 2012.

[6] B. D. Nguyen, K. T. Pham, V.-S. Tran, L. Mai, N. Yonemoto, A. Kohmura, et al., "Electronically tunable reflectarray element based on C-patch coupled to delay line," *Electronics Letters*, vol. 50, pp. 1114-1116, 2014.

[7] G. Perez-Palomino, R. Florencio, J. A. Encinar, M. Barba, R. Dickie, R. Cahill, et al., "Accurate and efficient modeling to calculate the voltage dependence of liquid crystal based reflectarray cells," 2014.

[8] K.-C. Lee and T.-N. Lin, "Application of neural networks to analyses of nonlinearly loaded antenna arrays including mutual coupling effects," *Antennas and Propagation, IEEE Transactions on*, vol. 53, pp. 1126-1132, 2005.

[9] D. Liao, "Scattering and imaging of nonlinearly loaded antenna structures in half-space environments," in *SPIE Defense, Security, and Sensing*, pp. 87140I-87140I-10, 2013.

[10] M. Bialkowski and H. Song, "Dual linearly polarized reflectarray using aperture coupled microstrip patches," in *Antennas and Propagation Society International Symposium, 2001, IEEE*, pp. 486-489, 2001.

[11] F. Venneri, S. Costanzo, G. Di Massa, and G. Amendola, "Aperture-coupled reflectarrays with enhanced bandwidth features," *Journal of Electromagnetic Waves and Applications*, vol. 22, pp. 1527-1537, 2008.

[12] P. Antognetti, G. Massobrio, and G. Massobrio, *Semiconductor Device Modeling with SPICE*, McGraw-Hill, Inc., 1993.

[13] S. A. Maas, *Nonlinear Microwave and RF Circuits*, Artech House, 2003.

[14] J. Huang, *Reflectarray Antenna*, Wiley Online Library, 2008.

Iman Aryanian was born in Iran in 1986. He obtained his B.Sc. in Electrical Engineering from Amirkabir University of Technology, Tehran, Iran in 2008, and the M.Sc. from Amirkabir University of Technology, Tehran, Iran in 2010. He is currently working toward his Ph.D. program. His research interests are in the areas of reflectarray antenna, computational electromagnetic, semiconductor RF modeling, electromagnetic theory, and computational electromagnetics.

Abdolali Abdipour was born in Alashtar, Iran, in 1966. He received his B.Sc. degree in Electrical Engineering from Tehran University, Tehran, Iran, in 1989, his M.Sc. degree in Electronics from Limoges University, Limoges, France, in 1992, and his Ph.D. degree in Electronic Engineering from Paris XI University, Paris, France, in 1996. He is currently a Professor with the Electrical Engineering Department, Amirkabir University of Technology (Tehran Polytechnic), Tehran, Iran. He has authored 5 books and has authored or co-authored over 290 papers in refereed journals and local and international conferences. His research areas include wireless communication systems (RF technology and transceivers), RF/microwave/millimeter-wave/THz circuit and system design, electromagnetic (EM) modeling of active devices and circuits, high-frequency electronics (signal and noise), nonlinear modeling, and analysis of microwave devices and circuits.

Gholamreza Moradi was born in Shahriar, Iran in 1966. He received his B.Sc. in Electrical Communication Engineering from Tehran University, Tehran, Iran in 1989, and the M.Sc. in the same field from Iran University of Science and Technology in 1993. Then he received his Ph.D. degree in Electrical Engineering from Tehran Polytechnic University, Tehran, Iran in 2002. His research areas include applied and numerical Electromagnetics, Microwave measurement and antenna. He has published more than fifty journal papers and has authored/co-authored five books in his major. He is currently an Associate Professor with the Electrical Engineering Department, Amirkabir University of Technology (Tehran Polytechnic), Tehran, Iran.